approximation with phase shifts derived fron ab initio calculations, using Hedin-Lundqvist potentials [P. A. Lee and J. B. Pendry, *Phys. Rev. B* **11**, 2795 (1975)]. The amplitude factor, AFAC in EXCURV92, was taken as 0.7 and not refined. The correction to the energy zero, E_f in EXCURV92, was refined to a value of −5.7 eV. We obtained a theoretical fit by adding shells of the backscattering atoms around the central Fe absorber and iterating the absorber-scatterer distances and Debye-Waller type factors. The latter included contributions from the thermal motion of the absorber-scatterer pairs and a static contribution from any variation in distance between the scatters in one shell. For the first shell only, we also iterated the number of backscatterers to find the best fit. The statistical test described by R. W. Joyner, K. J. Martin, and P. Meehan [*J. Phys. C* **20**, 4005 (1987)] indicated an improvement in the fit index at the 1% significance level on addition of the second shell.

15. B. A. Averill, T. Herskovitz, R. H. Holm, J. A. Ibers, *J. Am. Chem. Soc.* **95**, 3523 (1973).
16. Iron K-edge positions (electron volts) from XANES data: FeS_2 (7.1) FeAsS (6.4), $FeAs_2$ (5.9), $FeCuS_2$ (6.9), Fe_3S_4 (6.7), $(Fe,Ni)_3S_4$ (7.1), $FeCu_5S_4$ (6.9), and amorphous FeS (6.8).
17. We carried out ^{57}Fe Mössbauer spectroscopy using a conventional constant acceleration spectrometer and a ^{57}Co source. We maintained samples at low temperature by using liquid-N_2 and liquid-He bath cryostats. We calibrated the spectra using an Fe metal foil at room temperature and plotted with the center of the Fe metal spectrum as the zero of the velocity axis. Reconstituted ferritin samples for ^{57}Fe Mössbauer spectroscopy were enriched with ^{57}Fe [E. R. Bauminger, P. M. Harrison, I. Nowik, A. Treffry, *Biochemistry* **28**, 5486 (1989)]. The samples were stored frozen in liquid N_2 until used.
18. T. G. St Pierre *et al.*, *Biochim. Biophys. Acta* **870**, 127 (1986); J. M. Williams, D. P. Danson, C. Janot, *Phys. Med. Biol.* **23**, 835 (1978); R. B. Frankel, G. C. Papaefthymiou, G. D. Watt, in *Mössbauer Spectroscopy Applied to Inorganic Chemistry*, vol. 2, G. J. Lond, Ed. (Plenum, New York, 1987), p. 273.
19. J. B. Goodenough and G. A. Fatseas, *J. Solid State Chem.* **41**, 1 (1982). Typical values for the isomer shifts of octahedral high-spin Fe-S compounds are approximately 0.4 mm s^{-1} for Fe(III) and 0.8 mm s^{-1} for Fe(II). Tetrahedral coordination of Fe to S ligand gives isomer shift values of approximately 0.2 mm s^{-1} [Fe(III)], 0.4 mm s^{-1} (Fe +2.5), and 0.6 mm s^{-1} [Fe(II)].
20. An isomer shift value of 0.48 mm s^{-1} could also be interpreted as Fe(III) coordinated to six S atoms within the 500–Fe atom core. However, a typical Fe–S bond length for octahedral geometry is 2.41 Å, which is significantly larger than the experimental value of 2.22 Å determined by EXAFS analysis.
21. R. Cammack, D. P. E. Dickson, C. E. Johnson, *Iron-Sulfur Proteins*, W. Lovenberg, Ed. (Academic Press, New York, 1977), vol. 3, pp. 283–330.
22. J. C. Ward, *Rev. Pure Appl. Chem.* **20**, 175 (1970).
23. R. H. Griffith and A. R. Morcorn, *J. Chem. Soc.* **1945**, 786 (1945); R. Schrader and C. Pietzsch, *Z. Chem.* **8**, 154 (1968).
24. A. H. Stiller, B. J. McCormick, P. Russell, P. A. Montano, *J. Am. Chem. Soc.* **100**, 2554 (1978). The 77 K spectrum of "Fe_2S_3" showed two quadrupole components with isomer shift values of 0.35 and 0.51 mm s^{-1} and with quadrupole splittings of 0.82 and 0.88 mm s^{-1}, respectively. The hyperfine field at 4.2 K was 25 T.
25. D. E. Canfield and R. A. Berner, *Geochim. Cosmochim. Acta* **51**, 645 (1987); W. dos Santos Afonso and W. Stumm, *Langmuir* **8**, 1671 (1992).
26. T. Douglas *et al.*, unpublished observations.
27. J. E. Beesley, *Proc. R. Microsc. Soc.* **20**, 187 (1985).
28. D. W. R. Hall, *Scand. J. Gastroenterol.* **24**, 3 (1989).
29. P. J. Ell and E. S. Williams, *Nuclear Medicine: An Introductory Text* (Blackwell Scientific, Oxford, 1981).
30. T. A. Kent, M. J. Quast, B. J. Kaplan, R. S. Lifsey, H. M. Eisenberg, *Magn. Reson. Med.* **13**, 434 (1990).

31. Postdoctoral support for the work of T.D. was provided by the Engineering and Physical Sciences Research Council, United Kingdom.

9 February 1995; accepted 11 May 1995

Dynamics of Carbonium Ions Solvated by Molecular Hydrogen: $CH_5^+(H_2)_n$ (n = 1, 2, 3)

D. W. Boo, Z. F. Liu, A. G. Suits, J. S. Tse,* Y. T. Lee*

The dynamics of the carbonium ion (CH_5^+), a highly reactive intermediate with no equilibrium structure, was studied by measuring the infrared spectra for internally cold $CH_5^+(H_2)_n$ (n = 1, 2, 3) stored in an ion trap. First-principle molecular dynamics methods were used to directly simulate the internal motion for these ionic complexes. The combined experimental and theoretical efforts substantiated the anticipated scrambling motion in the CH_5^+ core and revealed the effect of the solvent molecular hydrogen in slowing down the scrambling. The results indicate the feasibility of using solvent molecules to stabilize the floppy CH_5^+ ion in order to make it amenable to spectroscopic study.

Protonated alkanes are highly reactive intermediates that form in the acid-catalyzed transformations of hydrocarbons as pioneered by Olah and co-workers (*1*). These carbonium ions are known to form a three-center, two-electron (3c2e) bond, which has pentacoordinated C atoms and bridged H atoms (*2*). The simplest carbonium ion, CH_5^+, has attracted considerable attention from both experimentalists and theoreticians during the last two decades (*3, 4*). Recent ab initio calculations at the most sophisticated level, performed by Schleyer, Schaefer, and co-workers (*5*), predicted the eclipsed C_s (e-C_s) symmetry to be the global minimum energy structure. However, the calculated energy differences between the e-C_s structure and others, such as the staggered C_s or C_{2v} structures, were very small and became negligible when corrected for zero-point vibrational energies. As emphasized by Scuseria (*6*, p. 512) recently, these results "clearly indicated that for all practical purposes CH_5^+ does not have a unique, stable equilibrium structure. The hydrogen atoms are predicted to scramble almost freely among multiple equivalent minima."

Studying the dynamics of such internal motion is quite challenging. Fourier transform ion cyclotron resonance mass spectrometry has been used experimentally to characterize indirectly the structure of CH_5^+, but the results were inconclusive (*3*). Many attempts have been made to obtain high-resolution infrared (IR) spectra for CH_5^+, with little success, probably because of the scrambling of CH_5^+ even at low temperatures, which caused significant spectral congestion. Theoretically, elucidation of the scrambling motion in CH_5^+ requires us to go beyond conventional quantum chemistry methods, which essentially treat a molecular or ionic system as a static entity. Molecular dynamics (MD) methods (*7*) would be ideal for such a floppy system, but unfortunately construction of a potential surface for such an ion with strong and complex chemical interactions is an almost impossible task.

We report an attempt to overcome these difficulties by a combination of state-of-the-art experimental and theoretical techniques. These efforts have been directed toward a study of the dynamics of the scrambling motion of core CH_5^+ in molecular hydrogen–solvated carbonium ions, $CH_5^+(H_2)_n$ (n = 1, 2, 3). The motivation was the notion that the interactions between the core CH_5^+ ions and the H_2 molecules are weak enough to cause only a minor perturbation to CH_5^+, yet strong enough to slow down the scrambling motions. Preliminary experimental results on $CH_5^+(H_2)$ (*8*) indicated the extensive scrambling of CH_5^+ and also some slowing of the scrambling by the solvent H_2, but the origin of these phenomena could not be determined because the spectral features were not resolved.

We used ion trap vibrational predissociation spectroscopy to measure the IR absorption of $CH_5^+(H_2)_n$ (n = 1, 2, 3). The experimental setup has been described in detail (*9*). Briefly, internally cold $CH_5^+(H_2)_n$ (n = 1, 2, 3) was produced from a high-pressure and low-current corona discharge source and subsequently was allowed to supersonically expand. The ion source was maintained at the optimum temperature for each kind of cluster ion to maximize the ion intensity. After several stages of ion optics to shape the beam, the ions were mass-selected by a 60° magnet sector analyzer, decelerated to a translation energy of ≤0.5 eV, and focused into a radio-frequency octapole ion trap. The ions were trapped there for ~2 ms, during which time the metastable ions decomposed and some radiative cooling took place for internally hot ions. The trapped, mass-selected ions were then vibrationally excited with a pulsed, tunable IR laser operating

---

D. W. Boo, Z. F. Liu, A. G. Suits, Y. T. Lee, Department of Chemistry, University of California, Berkeley, CA 94720, USA, and Chemical Sciences Division, Lawrence Berkeley Laboratory, 1 Cyclotron Road, Berkeley, CA 94720, USA.

J. S. Tse, Steacie Institute for Molecular Sciences, National Research Council of Canada, Ottawa, Ontario K1A 0R6, Canada.

*To whom correspondence should be addressed.

between 2600 and 3200 cm^{-1}. When an IR photon was absorbed, $CH_5^+(H_2)_n$ ($n = 1, 2, 3$) vibrationally predissociated into CH_5^+ and nH_2. The ions were then extracted and filtered by a quadrupole mass spectrometer tuned to pass only the daughter ions CH_5^+, which were then detected by a Daly ion detector (*10*). The intensity of the CH_5^+ signal as a function of laser frequency was a measure of the IR absorption of $CH_5^+(H_2)_n$ ($n = 1, 2, 3$). This combination of a cold ion source and an ion trap made possible the direct spectroscopic measurement on internally cold $CH_5^+(H_2)_n$ ($n = 1, 2, 3$) ions exclusively (*11*).

In theoretical calculations, we used first-principle MD methods to simulate $CH_5^+(H_2)_n$ ($n = 1, 2, 3$) dynamics at finite temperatures. Pioneered by Car and Parrinello, this method calculates the potential energy and forces on atoms, within the framework of local density functional theory, at each point along the classical Newtonian trajectory (*12*). Very recently this method was successfully applied to floppy ions such as CH_5^+ and $C_2H_3^+$ (*13*). In our calculations, a complex ion was seated in a face-centered cubic lattice cell with a lattice parameter of 30 atomic units, so that a plane wave basis set can be used when the interaction between ions in adjacent sites is negligible. The cutoff energy of the plane wave basis set was 20.0 rydberg. Vanderbilt-type pseudopotentials were used for both C and H atoms. Direct simulation of the internal motion for $CH_5^+(H_2)_n$ ($n = 1, 2, 3$) gave considerable insights into the solvation effects of H_2 for CH_5^+.

The experimental IR spectra for $CH_5^+(H_2)_n$ ($n = 1, 2, 3$) (Fig. 1) show spectral features due to C–H stretching modes in the core CH_5^+. Three stretching bands were predicted by ab initio calculations (*14*) in this frequency range, and the solid lines in Fig. 1 are the results of a least squares fit with three gaussian peaks shown as dashed lines. These peaks are fairly broad, indicating spectral congestion due to the scrambling motions of the core CH_5^+. However, as the number of solvent H_2 molecules increases, the IR spectra become better resolved. The trend seems to indicate that the scrambling motion in core CH_5^+ slows down as more H_2 molecules are attached to it.

First-principle MD results corroborate the experimentally observed trend. The evolution of H–H distance during 40,000 time steps (a total of ~3 ps) of simulation for $CH_5^+(H_2)_n$ ($n = 0$ to 3) is shown in Fig. 2. The temperature of these simulations was about 100 K, corresponding to an average internal energy of 0.3 kcal/mol, calculated from ab initio frequencies (*5*, *14*, *15*). The structure shown in Fig. 2A is an e-C_s structure and can be used as a reference for discussion, although CH_5^+ was not restricted to this structure. Hydrogen atoms H1, H2, and H4 formed three strong C–H bonds, whereas H3 and H5 formed a 3c2e bond with the C atom. This electron-deficient 3c2e bond was characterized by a short H–H distance (<1.5 Å). During the entire simulation, all H–H distances fluctuated between 1.0 and 2.2 Å, and the 3c2e bond could be formed between any pair of H atoms, in agreement with the theoretical predictions that CH_5^+ does not have a stable structure (*5*).

For $CH_5^+(H_2)$ (Fig. 2B), the CH_5^+ core remains floppy. For example, both H3–H4 and H3–H1 distances showed considerable fluctuations similar to those observed for CH_5^+. However, during the entire simulation the H_2 molecule was always bound to the H3 atom. Moreover, when Min(H3–H*n*), which is the minimum value of the distances between H3 and any one of the other H atoms in the CH_5^+ core, was compared with the corresponding Min(H1–H*n*), the former fluctuated much less and had a smaller average value than the latter. This finding indicates that the 3c2e bond is somewhat localized around H3, a slight yet interesting change in the scrambling motion of the CH_5^+ core.

For $CH_5^+(H_2)_2$ (Fig. 2C), the stabilization effect of two weakly bound H_2 molecules becomes more prominent. The two H_2 molecules were always bound to H1 and H2 of the core CH_5^+, respectively, and the H1–H2 distance stayed at around 1.25 Å with markedly small fluctuations (±0.05 Å root mean square). This result suggests that the 3c2e bond is localized to the C atom and the two H atoms weakly bonded to the two solvent H_2 molecules. This result could be attributed to the elec-

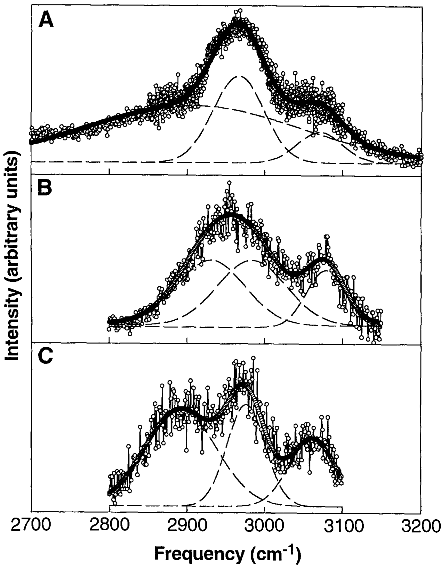

Fig. 1. Experimental IR spectra of $CH_5^+(H_2)_n$ (n = 1, 2, 3) for the C–H stretching modes: (**A**) $CH_5^+(H_2)$; (**B**) $CH_5^+(H_2)_2$; and (**C**) $CH_5^+(H_2)_3$.

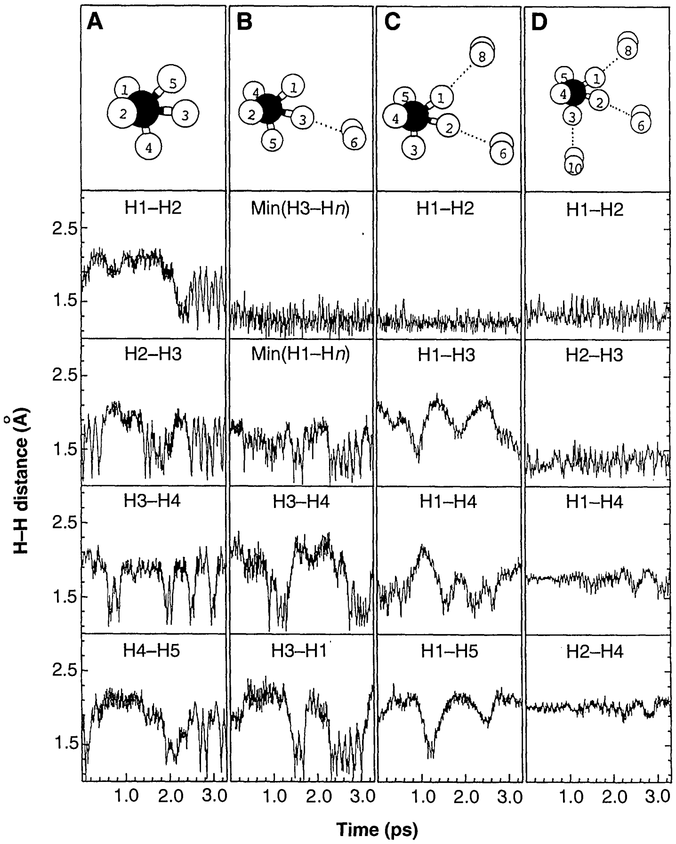

Fig. 2. Evolution of the H–H distances in the CH_5^+ core during the first-principle MD simulations: (**A**) CH_5^+; (**B**) $CH_5^+(H_2)$; (**C**) $CH_5^+(H_2)_2$; and (**D**) $CH_5^+(H_2)_3$. The hydrogen atoms on CH_5^+ are numbered 1 through 5, and the solvent H_2 molecules are labeled 6, 8, and 10.

tron deficiency in the 3c2e bond, which attracts the two solvent H_2 molecules. In contrast, the other three H atoms continued to go through large-amplitude motions such as CH_3 internal rotation, as indicated by the large fluctuations in the H1–H*n* distance in Fig. 2C.

For $CH_5^+(H_2)_3$ (Fig. 2D), the CH_5^+ core becomes semirigid. Three H_2 molecules were bound to H1, H2, and H3 in the CH_5^+ core, respectively, during the entire simulation. The in-plane wagging motion of H2 between H1 and H3 contributed to the slightly larger fluctuations in the H1–H2 and H2–H3 distances than in the H1–H2 distance for $CH_5^+(H_2)_2$. However, the fluctuations in the H1–H4 and H2–H4 distances were only 0.4 Å, indicating a considerable slowdown in the CH_5^+ scrambling motion and in agreement with the experimentally observed trend.

Our understanding of the IR spectra shown in Fig. 1 was facilitated by the insight that we obtained into the dynamics of the scrambling motion as discussed above and by comparison of the experimental spectra with the computed power spectra for $CH_5^+(H_2)_n$ (n = 1, 2, 3). The power spectra, obtained from the first-principle MD simulations, are plotted in Fig. 3 with the vibrational density of states as a function of frequency. Anharmonic coupling, which is very important for the floppy CH_5^+ yet difficult to account for in ab initio calculations, is naturally included in a power spectrum calculated by the Fourier transform of the velocity correlation function (*7*). For $CH_5^+(H_2)$, in spite of the stabilization effect of H_2, the CH_5^+ remained very floppy, and strong anharmonic couplings among vibrational modes were expected. Nonetheless, the center of the experimental spectrum at 2965 cm^{-1} was red-shifted only 27 cm^{-1} from the average C–H stretching frequency of CH_4 (2992 cm^{-1}), reflecting the fact that, when an H atom in CH_5^+ does not participate in the 3c2e bond, its corresponding C–H bond is similar to the C–H bond in CH_4. The three features in the power spectrum (Fig. 3A) could be correlated with the broad feature with two shoulders in the experimental spectrum (Fig. 1A). The calculated frequencies were ~10% lower than the experimental values. This discrepancy was likely due to slight imperfections in the pseudopotential. Mismatch in the intensities could be due to the fact that the plot shown in Fig. 3 is for density of states rather than for IR intensity.

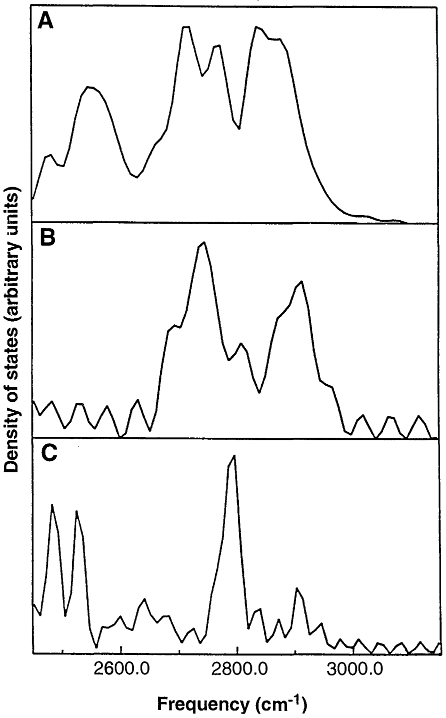

Fig. 3. Power spectra obtained from the first-principle MD simulations: (**A**) $CH_5^+(H_2)$; (**B**) $CH_5^+(H_2)_2$; and (**C**) $CH_5^+(H_2)_3$.

For $CH_5^+(H_2)_2$, the 3c2e bond was localized to H1–C–H2, which slowed the scrambling of the CH_5^+ core considerably. However, the scrambling of the other three C–H bonds was still extensive, and strong anharmonic couplings for the vibrational modes involving these three bonds were again expected. Two features were observed in the IR spectrum of $CH_5^+(H_2)_2$ (Fig. 1B), and the low-frequency shoulder observed for $CH_5^+(H_2)$ was no longer present. The broad and intense feature, centered at 2957 cm^{-1}, could be due to two strongly coupled C–H stretching modes, whereas the narrow feature, centered at 3078 cm^{-1}, could be due to another less coupled C–H stretching mode. The power spectrum for $CH_5^+(H_2)_2$ (Fig. 3B) was in especially good agreement with experiment (Fig. 1B).

For $CH_5^+(H_2)_3$, the CH_5^+ core was semirigid with internal scrambling considerably hindered. The presence of three partially resolved features in the experimental IR spectrum (Fig. 1C) is also suggestive of the semirigid nature of the CH_5^+ core in $CH_5^+(H_2)_3$. The observed frequencies (2892, 2977, and 3062 cm^{-1}) match well with the three ab initio CH_3 stretching frequencies, for e-C_s CH_5^+ (2891, 2993, and 3079 cm^{-1}) (*5*) and e-C_s $CH_5^+(H_2)$ (2898, 2998, and 3081 cm^{-1}) (*14*). These results suggest that the CH_5^+ core in $CH_5^+(H_2)_3$ has an e-C_s structure. The power spectrum for $CH_5^+(H_2)_3$ in Fig. 3C shows one sharp feature around 2800 cm^{-1} and two sharp features around 2500 cm^{-1}. The discrepancy is due to the fact that the 3c2e bond was quite delocalized in our simulation, a consequence of underestimation of the potential barrier for the in-plane wagging motion of H2 between H1 and H3 (see Fig. 2D). Preference for the delocalized 3c2e bond in CH_5^+ has also been observed in our earlier density functional quantum chemistry calculations (*15*).

This work can be extended in two ways. First, a high-resolution study on the vibration-rotational transitions of the solvent molecules in $CH_5^+(H_2)_n$ (n = 1, 2, 3) will give additional information on the structure and dynamics of CH_5^+, because the vibrational transitions are not strongly coupled to the floppy CH_5^+ core but still sample the structural parameters of the core ion. Second, inclusion of gradient correction in the local density functional calculation embedded in the first-principle MD simulation may improve the accuracy of the potential energy and of the simulation results.

REFERENCES AND NOTES

1. G. A. Olah, G. K. S. Prakash, J. Sommer, *Superacids* (Wiley-Interscience, New York, 1985).
2. G. A. Olah, *Carbocations and Electrophilic Reactions* (Verlag Chemie, Weinheim, Germany, 1973).
3. M. D. Sefcik, J. M. S. Henis, P. P. Gasper, *J. Chem. Phys.* **61**, 4321 (1974); R. D. Smith and J. H. Futrell, *Chem. Phys. Lett.* **36**, 545 (1975); A. J. R. Heck, L. J. de Koning, N. M. M. Nibbering, *J. Am. Soc. Mass Spectrum.* **2**, 453 (1991).
4. V. Dyczmons, V. Staemmler, W. Kutzelnigg, *Chem. Phys. Lett.* **5**, 361 (1970); W. A. Lathan, W. J. Hehre, L. A. Curtiss, J. A. Pople, *J. Am. Chem. Soc.* **93**, 6377 (1971); K. Ragavachari, R. A. Whiteside, J. A. Pople, P. v. R. Schleyer, *ibid.* **103**, 5649 (1981); K. Hirao and S. Yamabe, *Chem. Phys.* **89**, 237 (1984); W. Klopper and W. Kutzelnigg, *J. Phys. Chem.* **94**, 5625 (1990).
5. P. R. Schreiner, S. J. Kim, H. F. Schaefer, P. v. R. Schleyer, *J. Chem. Phys.* **99**, 3716 (1993); P. v. R. Schleyer and J. W. M. Carneiro, *J. Comput. Chem.* **13**, 997 (1992).
6. G. E. Scuseria, *Nature* **366**, 512 (1993).
7. M. P. Allen and D. J. Tildesley, *Computer Simulation of Liquids* (Oxford Univ. Press, Oxford, 1987).
8. D. W. Boo and Y. T. Lee, *Chem. Phys. Lett.* **211**, 358 (1993).
9. S. W. Bustamente, thesis, University of California, Berkeley (1983).
10. R. N. Daly, *Rev. Sci. Instrum.* **31**, 264 (1960).
11. The larger complexes such as $CH_5^+ (H_2)_n$ (n = 4, 5, 6) have also been isolated and studied in a similar manner. The vibrational spectra were similar to that for $CH_5^+(H_2)_3$, suggesting that the scrambling of the CH_5^+ core was more or less frozen at n = 3.
12. R. Car and M. Parrinello, *Phys. Rev. Lett.* **55**, 2471 (1985); D. K. Remler and P. A. Madden, *Mol. Phys.* **70**, 921 (1990).
13. J. S. Tse, D. D. Klug, K. Lassonen, *Phys. Rev. Lett.* **74**, 876 (1995).
14. S. J. Kim, P. R. Schreiner, P. v. R. Schleyer, H. F. Schaefer, *J. Phys. Chem.* **97**, 12232 (1993).
15. D. W. Boo and J. S. Tse, unpublished results.
16. Supported by the Director, Office of Energy Research, Office of Basic Energy Sciences, Chemical Sciences Division of the U.S. Department of Energy under contract DE-AC03-76SF00098. Z.F.L. is a Natural Sciences and Engineering Research Council (Canada) postdoctoral fellow. Part of the simulation reported was performed on the Cray-90 at the National Energy Research Supercomputing Center.

27 February 1995; accepted 16 May 1995